ACADEMIC PRESS

Available online at www.sciencedirect.com
SCIENCE DIRECT®

Journal of Catalysis 214 (2003) 1–7

JOURNAL OF CATALYSIS

www.elsevier.com/locate/jcat

Propene hydrogenation over truncated octahedral Pt nanoparticles supported on alumina

Jung Whan Yoo, David J. Hathcock, Mostafa A. El-Sayed *

Laser Dynamics Laboratory, School of Chemistry and Biochemistry, Georgia Institute of Technology, Atlanta, GA 30332-0400, USA

Received 17 September 2001; revised 12 July 2002; accepted 7 August 2002

Abstract

Colloidal Pt nanoparticles synthesized by a 1 : 5 concentration ratio of K_2PtCl_4 to polyacrylate were loaded on nanoporous alumina using the impregnation method at room temperature. The deposited Pt particles, present on the external surfaces of the support, were characterized by transmission electron microscopy, which indicated predominantly truncated octahedral (TO) shapes with a mean diameter of 10 nm. Their catalytic performance in the hydrogenation of propene at 30–80 °C was studied as a test reaction. The initial rate, reaction order, rate constant, activation energy, and turnover frequency were determined. The activation energy was found to be 8.4 ± 0.2 kcal/mol, which is slightly lower than results reported for other platinum systems (10–14 kcal/mol). The TO platinum nanoparticles have atom-high surface steps, ledges, and kinks, and these atomic-scale fine structures are expected to decrease the activation energy. The reactivity of the surface atoms in this nanoparticle is so high that above 50 °C side reactions leading to complete surface poisoning take place within a few minutes. The effect of the polymer concentration of the polyacrylate-capped TO Pt/Al_2O_3 on the hydrogenation catalytic activity was also investigated.

Keywords: Platinum; Truncated octahedral; Nanoparticle; Alumina; Propene; Hydrogenation; Activation energy; Transmission electron microscopy; FT-IR

1. Introduction

Transition metals have long been used in the catalysis field [1–15]. Catalysis on transition metal surfaces is a field rich in activity and experiments have been carried out as early as 1823 [14,15]. However, active studies on catalysis with nanoparticle surfaces is a very young field but research in this area is increasing almost exponentially [16].

Nanometer-sized colloidal metal particles are of great interest in modern chemical research, where they find application in such diverse fields as photochemistry [17], electrochemistry [17–19], optics [17–21], and catalysis [16,17,22]. The chemical and physical properties of these particles are distinct from those of the bulk phase and those of isolated atoms and molecules. In relation to catalysis, this difference was noted very early and has been the subject of early studies [23,24]. The specific properties of nano-sized metal particles in catalysis are usually associated with a change in their electronic properties relative to the bulk samples. This change is a result of size effects, giving rise to an increase in the surface energy and a characteristic high surface-to-volume ratio. These lead to an enhancement of the particles' catalytic properties [25] because large fractions of the active metal atoms are on the surface and thus are accessible to reactant molecules and available for catalysis [26]. For these reasons, many workers have synthesized platinum nanoparticles deposited on inorganic materials as used in heterogeneous catalysis for use in various reactions [27–30]. These catalysts are typically prepared without capping materials by impregnation/ion-exchange methods using various Pt precursors such as H_2PtCl_6 [27], $Pt(NH_3)_4(NO_3)_2$ [28], $Pt(AcAc)_2$ [28], $Pt(NH_3)_4Cl_2$ [29], $Pt(NH_3)_4(OH)_2$ [12], and $Pt(allyl)_2$ [30], which give mainly amorphous (shapeless) nanoparticles.

Generally, the particle sizes and the dispersion states of metal nanoparticles are important factors in explaining their catalytic property. A relationship between the size of copper nanoparticles and the catalytic activity evaluated by hydration of unsaturated nitriles was reported by Hirai et al. [31]. They attributed the increase in the catalytic activity to an

* Corresponding author.
E-mail address: mostafa.el-sayed@chemistry.gatech.edu (M.A. El-Sayed).

0021-9517/03/$ – see front matter
doi:10.1016/S0021-9517(02)00136-7

increase in the surface area of the nanoparticles due to the decrease of the particle size. However, the opposite result was also reported [32]. An enhancement of both the specific activity and the turnover frequency was observed on the large silver particles compared with the small silver particles in the hydrogenation of crotonaldehyde. In addition, the selectivity to the unsaturated alcohol is found to increase with increasing silver particle size [32]. This catalyst gave a higher selectivity to crotyl alcohol (53%) than the ultradispersed small silver particles, which produced crotyl alcohol with a selectivity of only 28%. These results indicate that the rate-determining step depends critically not on the surface areas and dispersion states but on the silver particle size and surface structure. As described by Claus and Hofmeister [32], the activity and selectivity of some reactions depend on the nature of the surface sites on the nanoparticles. Factors which determine the coordination of surface metal atoms depend on size, shape, exposed facets, and surface roughness [33].

The dependence of the selectivity and activity on the substrate surface has been well known for many years. A variety of different surface reactions have shown a large dependence not only on the surface roughness of the catalyst but also on the crystal lattice. This has been shown for single-crystal platinum samples under UHV conditions by a number of groups and in several early works for dispersions of colloidal transition metals.

Capping material (e.g., polymer) is added to the suspension to prevent coagulation and precipitation of the metal nanoparticles. A portion of the added polymer exhibits a protective function by the adsorption of the polymer onto the metal nanoparticles; the other portion of the polymer dissolves freely in the suspension of the metal nanoparticles. Both the amount of the polymer adsorbed on metal nanoparticles and the concentration of free polymer are important for the application of the metal nanoparticles. However, there have been no reports on correlation of the catalytic activity with either the amount of the polymer adsorbed on metal nanoparticles or the concentration of free polymer in catalysts.

In the present study, truncated octahedral (TO) platinum nanoparticles are synthesized using K_2PtCl_4 solution and polyacrylate as the capping material and impregnated on an alumina support. The particle size/shape are characterized by transmission electron microscopy (TEM). The catalytic activity is measured by the values of the activation energy and the turnover frequency as studied for the heterogeneous hydrogenation of propene. Quantities of the polyacrylate on TO platinum deposited on alumina are determined by FT-IR and are qualitatively correlated to the catalytic activity of the hydrogenation.

2. Experimental

2.1. Chemicals

K_2PtCl_4 (99.99%), sodium polyacrylate (average MW 2100), and alumina (neutral, surface area of 155 m^2/g, pore size of 5.8 nm) were obtained from Aldrich. All solutions were prepared using doubly deionized water. Propene (99.9995%) and hydrogen (99.995%) were purchased from Matheson and were used without further purification. The purity of the propene was checked by mass spectrometry.

2.2. Catalyst preparation

The platinum deposited on alumina (Pt/Al_2O_3) catalyst was prepared as follows. The platinum nanoparticles were synthesized in aqueous solution by using the methods reported by Rampino and Nord [23] and Henglein et al. [34]. One ml of 0.1 M sodium polyacrylate as a capping polymer was added to 250 ml containing 8.0×10^{-5} M K_2PtCl_4 solution. The initial concentration ratio of K_2PtCl_4 to polyacrylate was 1 : 5. The pH or the solution was adjusted to 7 with 0.1 M HCl and purged with Ar for 20 min. The platinum complexes were reduced by bubbling with H_2 for 5 min. The solution was left for 12 h in the dark. Alumina (5 g) was added to this solution and was impregnated using rotary evaporation at room temperature under reduced pressure. Finally, the catalyst was dried at 110 °C for 12 h.

2.3. TEM and FT-IR measurements

TEM was used to determine the particle size and shape of the platinum nanoparticles supported on alumina. For TEM sample preparation, the Pt/Al_2O_3 catalyst was suspended in deionized water by ultrasonification for 1 h after grinding of the Pt/Al_2O_3 and was subsequently left for several hours. The suspended sample was deposited on a carbon grid and was left to dry slowly at room temperature. TEM images were taken by using a JEM 100C operated at an acceleration voltage of 100 kV at a magnification of 100,000–190,000 at room temperature. The particle size and shape were determined from enlarged TEM images.

FT-IR spectra were recorded from pellets of the sample using a Bruker IFS 66/S FT-IR spectrometer. Typically, 100 scans were accumulated for each spectrum with a resolution of 2 cm^{-1} using Bruker's OPUS 2.0 software. FT-IR spectra were recorded in the range of 2300–1000 cm^{-1}. Static pressure was applied to the powder sample until the pellet made a clear disk.

3. Results and discussion

3.1. TEM images of platinum nanoparticles deposited on alumina

In general, structure characterization of real catalysts by electron microscopy is complicated by the strong contrast features originating from the support material, by the random orientation of metal particles, and by superposition of particle images due to the nonplanar morphology of the catalyst [35]. Where the support is thick, it is not possible to see the metal particles at all through the support. It is difficult, therefore, to determine clear structural features such as particle size and shape. Figure 1 shows TEM pictures of Pt/Al_2O_3 in which the platinum particles were synthesized with a 1 : 5 concentration ratio of K_2PtCl_4 to polyacrylate followed by impregnation of alumina with the platinum solution at room temperature under atmospheric pressure. The platinum particles in aqueous solution at 60–80 °C are observed to aggregate during impregnation. As can be observed in the TEM pictures, the platinum particles that are supported on alumina show clear images even in the presence of alumina. The nanoparticles are randomly distributed on the support and 90% of them are found to have a TO shape with a size range of 8–10 nm. This result is in good agreement with those obtained in the absence of alumina and reported by our group [36]. The particle size of the TO platinum is larger than the alumina pore aperture (5.8 nm), from which it can be concluded that the nanoparticles are located on the external surfaces of the alumina support.

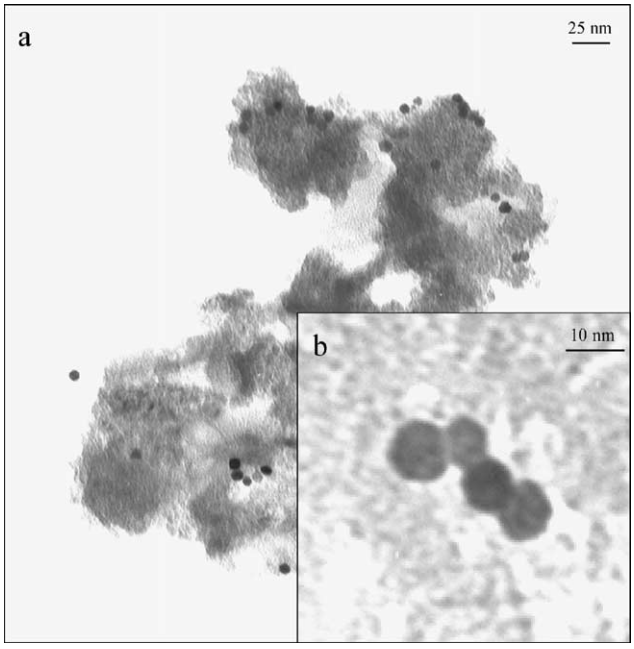

Fig. 1. TEM images of (a) TO Pt/Al_2O_3, synthesized with a concentration ratio of 1 : 5 platinum complex to polyacrylate following impregnation on alumina and (b) enlargement of TO Pt/Al_2O_3.

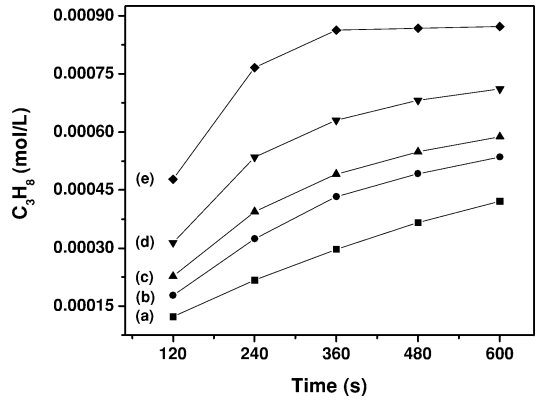

Fig. 2. Propane concentration for temperature-dependant propene hydrogenation over TO Pt/Al_2O_3 catalyst as a function of reaction time: (a) at 30 °C, (b) at 40 °C, (c) at 50 °C, (d) at 60 °C, and (e) at 70 °C.

3.2. Catalysis of propene hydrogenation

To evaluate the catalytic activity of the nanoparticles, the hydrogenation of gaseous propene was selected as a test reaction. The propene hydrogenation was carried out in a batch reactor. Prior to the reaction, the catalyst was preheated to 210 °C for 2 h under an Ar flow and then was evacuated under high vacuum at this temperature for 10 min. This treatment is carried out to remove the capping material, water, and volatile impurities [37].

The hydrogenation experiments were typically run in the presence of 0.12 g of TO Pt/Al_2O_3 mixture which is 0.078% by weight platinum. Propene (24 Torr) and hydrogen (165 Torr) were then added and the mixture was heated to the specified temperature in the 30–80 °C range. Aliquots of the reaction mixture were taken out at different reaction times and were analyzed by mass spectrometry (VG Analytical, 70-SE). The relative intensities of propane to propene mass peaks in the hydrogenation reaction were calibrated from known standard propene/propane gas mixtures. The relative mass peak intensities of propene to propane, observed at each time during the catalyzed reaction, were converted to concentration by using a predetermined calibration curve.

The kinetic studies were carried out in the following manner. First, propane concentration vs time is plotted at each temperature studied (Fig. 2). The reaction rates as a function of time are determined from the tangent of the slopes of the plots at different reaction times. These rates are then plotted vs time to determine the initial rates for each temperature by extrapolating to zero time (Fig. 3). The reaction order for each of the reactants (the propene and hydrogen) and thus the rate law are obtained from the dependence of the initial rates on the concentration of H_2 and propene at 40 °C. The rate constant (k) at different temperatures is then calculated from the initial reaction rate, the rate law, the corrected initial H_2, and propene concentrations at each temperature. An Arrhenius plot is then used to determine the value of the activation energy (Fig. 4).

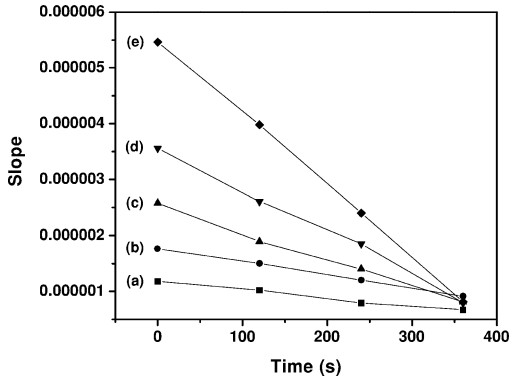

Fig. 3. Slope of propane concentration for temperature-dependant propene hydrogenation over TO Pt/Al_2O_3 catalyst as a function of reaction time: (a) at 30 °C, (b) at 40 °C, (c) at 50 °C, (d) at 60 °C, and (e) at 70 °C.

The hydrogenation reaction on platinum catalyst is well studied in terms of specific catalytic activity, kinetic reaction law, and activation energy [38,39]. However, the effects of platinum nanoparticle shape and capping material on the value of the activation energy in the propene hydrogenation have not been studied. Under our mild reaction conditions, propane is the only reaction product detected by the mass spectrometer. These observations are in agreement with the work of Bond [40], who has shown that platinum metal is an effective catalyst to selectively convert propene to propane.

Figure 2 shows a plot of propane concentration vs reaction time in the propene hydrogenation over TO Pt deposited on alumina in the temperature range of 30–80 °C. The propane concentration is found to increase almost linearly with time in the range of 30–50 °C, but in the 60–80 °C range, the concentration tends to level off slowly and almost reaches a constant value within 8 min. The slope (tangent) of these curves at any time gives the instantaneous rate of the reaction at this time. To determine the initial rate, these slopes are plotted as a function of time and are extrapolated to zero time at each temperature. The results are shown in Fig. 3 and the calculated initial rates at different temperatures are given in Table 1. From Fig. 3 it is obvious that above 50 °C, the apparent rate of

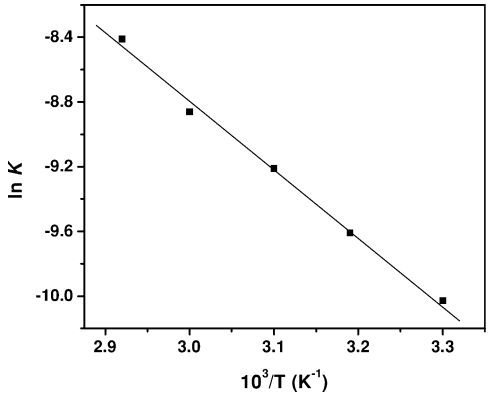

Fig. 4. Arrhenius plots of the propene hydrogenation over TO Pt/Al_2O_3 catalyst.

Table 1
Initial rates and rate constants of propene hydrogenation over truncated octahedral Pt/Al_2O_3 thermally pretreated at 210 °C at different temperatures

$T(K)$	Initial rate ($\times 10^{-6}$ mol L^{-1} s^{-1})	$[C_3H_6]_{Initial}$ ($\times 10^{-3}$ M)	$[H_2]_{Initial}$ ($\times 10^{-3}$ M)	Rate constant ($\times 10^{-4}$)
303	1.18	1.27	8.73	0.44
313	1.76	1.23	8.45	0.67
323	2.58	1.19	8.19	1.0
333	3.56	1.16	7.95	1.42
343	5.46	1.12	7.71	2.22

production of propene drops to almost zero in ∼ 8 min. The apparent constancy of the product could be due to the mixture reaching equilibrium in which the rate of the dehydrogenation of propane becomes equal to the forward hydrogenation reaction. It could also result from poisoning of the catalyst surface. The fact that we did not observe any dehydrogenation of propane on this catalyst at these temperatures suggests that the surface gets poisoned due to secondary reactions that become fast at temperatures higher than 50 °C. It is well known that Pt single-crystal catalysts involved in hydrogenation reactions can build up carbonaceous deposits on the surface leading to deactivation [41,42]. UHV studies by Somorjai et al. have found that these layers build up on the surface and can interfere with the hydrogenation of organic molecules [42]. Because of the similarities between the hydrogenation of propene and the hydrogenation reaction of ethylene, such a process could conceivably occur at the surface of the nanoparticles. In the case of small nanoparticles, the highly active nature of the surface could make them more susceptible to this type of poisoning.

The reaction is assumed to follow the reaction rate law

$$\text{Initial reaction rate} = k[C_3H_6]^{\alpha}[H_2]^{\beta},$$

where α and β are the order of the reaction with respect to C_3H_6 and H_2, respectively. By determining the initial rates at different reactant concentrations, α and β are found to be 0.13 and 0.58, respectively. These values are quite similar to those reported by Cocco et al. [43] for the catalysis using Pt on SiO_2 and TiO_2, suggesting a similar mechanism.

The specific rate constant k at different temperatures is calculated from these initial reaction rates, the reaction order, and the corrected initial H_2 and propene concentrations at the different temperatures. This is shown in Table 1. Figure 4 gives the Arrhenius plot of the natural logarithm of the rate constant vs $1/T$ for the reaction catalyzed by TO Pt/Al_2O_3. As shown, normal Arrhenius behavior is observed in the temperature range of 30–80 °C. The activation energy of the reaction is calculated to be 8.4 ± 0.2 kcal/mol from the observed slope of the linear part of the Arrhenius plot. The fact that all the points fall on the same straight line, even the ones above 50 °C, suggests that the initial rates represent the hydrogenation reaction. The secondary reactions, leading to surface poisoning, build up at slightly longer times than zero time.

Other groups [43,44] have reported the activation energy and reaction orders with respect to propene and hydrogen in the propene hydrogenation catalyzed by platinum supported on silica and titania. The supported platinum particles have been prepared by impregnation/ion-exchange methods by immersing the calcined supports in an aqueous or organic solution of platinum precursors such as H_2PtCl_6 [44] and $Pt(allyl)_2$ [43], without the addition of capping material. The platinum catalysts are reduced in flowing hydrogen at about 450 °C. These methods typically give amorphous nanoclusters, although there is no detailed description about the particle shapes. Reviewing the work on propene hydrogenation shows that the reaction orders for propene and hydrogen converge to 0 and 0.5, respectively, and the activation energy ranges from 10 to 14 kcal/mol [43,44]. The activation energies were found to depend on the type of support (silica, titania) and the structure (anatase, rutile) due to the different interactions between the platinum and the support giving different electronic effects [43,44]. Otero-Schipper et al. [44] showed that the activity increases as the percentage of platinum exposed increases. The fact that the activation energy is independent of the percentage of platinum exposed while the overall activities vary suggests an activity compensation in which variations in the activity are due to variations in the preexponential factor. Thus Otero-Schipper et al. correlated the activity measured by the turnover frequency (TOF) to the fraction of atoms on edges and corners of the exposed crystallite. They found that the turnover frequency increases linearly as the ratio of edge and corner atoms to total exposed atoms increases. It is believed that, in general, the chemical activities of platinum particles with different shapes are sensitive not only to the surface facets but also to the atomic structures, such as steps, ledges, and defects [45]. The TO platinum nanoparticles are mainly defined by the {100}, {111}, and {110} facets, on which numerous atom-high surface steps, ledges, and kinks have been observed [45]. These atomic-scale fine structures of the surfaces of the TO platinum nanoparticles are expected to have lower activation energy than those reported by others.

The TOF was calculated by determining the moles of product produced (or reactant consumed) per unit time per mole of available active sites on the catalyst. This can be obtained from the initial rate multiplied by the reaction volume and divided by the moles of active surface sites. The latter is difficult to determine exactly, even if one determines the moles of binding sites for a certain gas. This is because these sites may be different from those that actually catalyze the reaction. In our work we assumed that our heating treatment completely removes the capping material. In addition, we assumed, as is done in many other publications [47,48], that the number of moles of surface atoms is equal to the number of moles of active sites. This will give us a lower limit for the TOF.

The particles are of a cubic close packed cuboctahedral structure. The cuboctahedra are made up of complete shells of atoms, the number of which can be calculated from known equations [46] and the TEM data of the average particle size. Using this geometric relationship, the number of total surface atoms per particle having an average radius determined from TEM can be calculated. The total number of moles of particles can be calculated from the assumption that all the atomic moles of platinum used in the synthesis were converted to nanoparticles of the average size determined by TEM. From the moles of surface atoms per particle and the number of moles of particles, the total number of moles of surface atoms can be calculated. The initial rate constant is then multiplied by reaction volume and divided by the total moles of surface atoms on all the particles used to obtain the TOF.

For quantitative understanding, the catalytic activity in terms of TOF is calculated and compared to that reported by others. Our catalyst shows TOF of 0.62 $\mathrm{mol_{C_3H_8}/mol_{Pt}}$ s at 70 °C. Although some workers have published papers about the hydrogenation of propene over platinum nanoparticles supported on inorganic materials, they did not give the catalytic activities in terms of TOF. Therefore, we compare our TOF to that obtained for similar reaction conditions using the same group metal, palladium. Ciebien et al. [49] synthesized palladium nanoclusters within diblock copolymer films and applied to the hydrogenation of propene. A maximum TOF of 0.021 $\mathrm{mol_{C_3H_8}/mol_{Pt}}$ s was obtained at 120 °C in a concentration ratio of 2 : 1 hydrogen to propene pressure. Our catalyst shows much higher activity. Although the deposited active metals are different, the reason might be ascribed to the surface irregularities, steps, ledges, and kinks of the TO platinum deposited. Of course, this high catalytic activity of our TO Pt particles is the reason for the rapid poisoning of the surface during the reaction.

Capping materials such as polyacrylate [36,50] and poly(*N*-vinyl-2-pyrrolidone) [51,52] have been typically used as stabilizers for protecting these nanoparticles against aggregation and as a controller of the platinum nanoparticle shapes (TO, cubic, and tetrahedral). This is controlled by changing the ratio of the concentration of the capping material to that of the platinum precursor. Although the capping material has advantages like those already described, it is expected that they have a negative effect due to the partial covering of the active sites of the nano-sized metal particles. Nevertheless, many studies have been carried out on the hydrogenation reaction over nanometal particles capped with polymers [51–53].

Polyacrylate-capped TO Pt/Al_2O_3 samples were studied by FT-IR before and after thermal treatment at 210 or 310 °C under the flow of argon to investigate the influence of the polymer quantity on the catalytic activity of the propene hydrogenation. The results are shown in Fig. 5. Polyacrylate (curve e in Fig. 5) has strong absorption bands at 1570 and 1406 $\mathrm{cm^{-1}}$ assigned to the asymmetric and symmetric stretching vibrations of the $\mathrm{COO^-}$ moiety, respectively. The peak at 1456 $\mathrm{cm^{-1}}$ is assigned to the CH_3 rocking vibration [54]. Characteristic bands of alumina (curve b) are observed at 1643 and 1400 $\mathrm{cm^{-1}}$, which

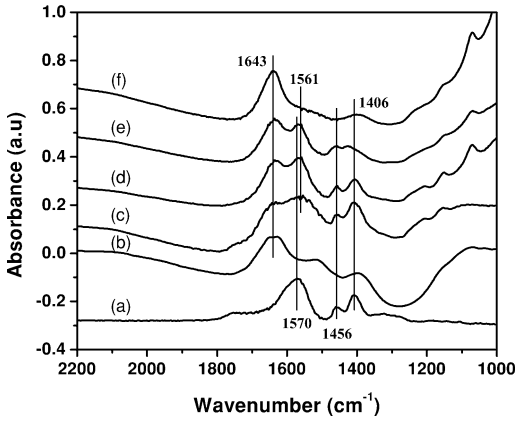

Fig. 5. FT-IR spectra of (a) polyacrylate, (b) alumina, (c) as-synthesized TO Pt/Al_2O_3, (d) heated (c) sample at 210 °C for 2 h under flowing argon and evacuated at same temperature for 10 min, (e) thermally treated (c) sample at same conditions as (d) sample except at 310 °C, and (f) thermally oxidized (c) sample at 310 °C for 2 h.

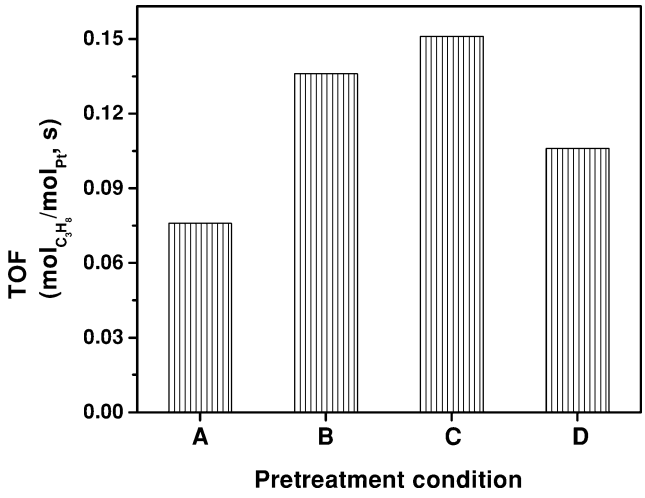

Fig. 6. Effect of catalyst pretreatment on catalytic activity (indicated at 30 °C for 4 min) over TO Pt/Al_2O_3; (A) as-synthesized TO Pt/Al_2O_3, (B) heated (A) sample at 210 °C for 2 h under flowing argon and evacuated at same temperature for 10 min, (C) thermally treated (A) sample at same conditions as (B) sample except at 310 °C, and (D) thermally oxidized (C) sample at 310 °C for 2 h.

are clearly resolved from the polymer bands. As-synthesized TO Pt/Al_2O_3 exhibits physisorbed and chemisorbed bands at 1570 and 1561 cm^{-1}, respectively, as shown in curve c of Fig. 5. From this observation, we conclude that some polymers act as a stabilizer to protect against aggregation through the chemical attachment of COO^- of the polyacrylate onto platinum nanoparticle surfaces. The others are physically adsorbed on the TO Pt/Al_2O_3. Curve d shows the FT-IR of the sample that was heated at 210 °C for 2 h with flowing argon gas followed by pumping under vacuum (10^{-3}–10^{-4} Torr) for 10 min. This shows the chemisorbed polymer bands with reduced intensity when compared to those of as-synthesized TO Pt/Al_2O_3. On the other hand, the physisorbed polymer is almost completely eliminated. The polyacrylate used for preparation of TO-shaped platinum nanoparticles was reported to be removed at 180 °C and the particle shape is not transformed until 350 °C [37]. This result is in contrast with that concluded from our FT-IR data. The reason might be that the TEM experiment was detecting the physisorbed polymer and could not detect the chemisorbed component. Furthermore, the high vacuum used (10^{-9}–10^{-11} Torr) might have been effective in removing a large fraction of the polymer. When the temperature was increased to 310 °C, the polymer remained due to the strongly bound chemisorbed polymer. However, when the sample was calcined under an air atmosphere at 310 °C for 2 h, the polymer bands were completely removed, as indicated in curve f of Fig. 5.

The TO Pt/Al_2O_3 catalysts treated under different conditions present different TOFs (indicated at 30 °C), depending on the quantity of the polymer (Fig. 6). The TOF obtained after thermal treatment at 210 °C is found to increase by about 80% compared to that of the as-synthesized catalyst. This is attributed to the complete removal of the physisorbed polyacrylate which covered the surface of the active site of platinum nanoparticles. The TO Pt/Al_2O_3 heated at 310 °C shows ∼ 11% enhancement over that heated at 210 °C. This is due to an increase in the exposed surface resulting from the dissociation of the chemisorbed polymer, as suggested by the FT-IR results. The polymer-removed TO Pt/Al_2O_3 by air calcination exhibits a 30% reduction in the catalytic activity compared to that treated in an argon gas atmosphere. This could be due to the possible oxidation of the platinum surfaces in the air-calcinated catalyst.

4. Conclusions

Platinum nanoparticles were synthesized by using K_2PtCl_4 in the presence of polyacrylate as capping material and were deposited on nanoporous alumina by impregnation at room temperature. TEM images showed that the nanoparticles have mainly a TO shape with size range of 8–10 nm. These are randomly dispersed on the external surface of alumina, since the particle size is larger than the alumina pore aperture (5.8 nm).

The TO Pt/Al_2O_3 catalyst was used for propene hydrogenation to evaluate its catalytic activity as measured by the value of its activation energy and TOF. The activation energy is found to be 8.4 ± 0.2 kcal/mol, which is lower than those values reported by others on other platinum particles (10–14 kcal/mol). However, for experiments above 50 °C, the activity of the particles degraded to zero after only a few minutes, suggesting a poisoning process on the surface of the particles. Both the lower activation energy and the rapid poisoning of the catalyst surface at $\geqslant 50$ °C suggest that Pt atoms on the surface of the TO nanocatalyst are very active (reactive). They might be due to the facets, edges, corners, and defects present in the TO nanoparticles.

Polyacrylate-capped TO Pt/Al_2O_3 samples, before and after thermal treatment, are characterized by FT-IR with

and without thermal treatment to investigate the influence of the polymer quantity on the catalytic activity of the hydrogenation reaction. Even under high vacuum at 310 °C, the chemisorbed polymer is found to be strongly bound to the surface or the particles. The catalytic activity increases as the amount of capping polymer is removed.

Acknowledgments

Financial support of this work was from the Julius Brown Chair Research Fund at Georgia Tech. We wish to thank Colin Heyes for proofreading the manuscript.

References

[1] G.A. Somorjai, Introduction to Surface Chemistry and Catalysis, Wiley, New York, 1994, pp. 1–17.
[2] I. Langmuir, J. Am. Chem. Soc. 40 (1918) 1361.
[3] R.P. Donnelly, C.N. Hinshelwood, J. Chem. Soc. 1727 (1929).
[4] C.N. Hinshelwood, R.E. Burk, J. Chem. Soc. 127 (1925) 2896.
[5] R.J. Breakspere, D.D. Eley, P.R. Norton, J. Catal 27 (1972) 215.
[6] D.D. Eley, Catal. Hydrogenation Dehydrogenation 3 (1955) 49.
[7] R.J. Mikovsky, M. Boudart, H.S. Taylor, J. Am. Chem. Soc. 76 (1954) 3814.
[8] K.E. Hayes, H.S. Taylor, Z. Phys. Chem. (Frankfurt) 15 (1958) 127.
[9] J.F. Woodman, H.S. Taylor, J. Turkevich, J. Am. Chem. Soc. 62 (1940) 1397.
[10] T. Tucholski, E.K. Rideal, J. Chem. Soc. 1701 (1935).
[11] E.K. Rideal, Chem. Soc. 121 (1922) 309.
[12] J. Addy, G.C. Bond, Trans. Faraday Soc. 53 (1957) 388.
[13] G.C. Bond, Trans. Faraday Soc. 52 (1956) 1235.
[14] J.W. Döbereiner, J. Chem. (Schweiger) 38 (1823) 321.
[15] J.W. Döbereiner, Ann. Phys. (Gilbert) 74 (1823) 269.
[16] J.D. Aiken III, R.G. Finke, J. Mol. Catal. A: Chem. 145 (1999) 1.
[17] J.S. Bradley, in: G. Schmid (Ed.), Clusters and Colloids, VCH, Weinheim, 1994, pp. 459–537.
[18] C.N.R. Rao, G.U. Kulkarni, P.J. Thomas, P.P. Edwards, Chem. Soc. Rev. 29 (2000) 27.
[19] G. Schmid, L.F. Chi, Adv. Mater. 10 (1998) 515.
[20] A. Henglein, Chem. Rev. 89 (1989) 1861.
[21] G. Schmid, Chem. Rev. 92 (1992) 1709.
[22] L.N. Lewis, Chem. Rev. 93 (1993) 2693.
[23] L.D. Rampino, F.F. Nord, J. Am. Chem. Soc. 63 (1942) 2745.
[24] G.C. Bond, Trans. Faraday Soc. 52 (1956) 1235.
[25] C.-B. Hwang, Y.-S. Fu, Y.-L. Lu, S.-W. Jang, P.-T. Chou, C.R. Wang, S.J. Yu, J. Catal. 195 (2000) 336.
[26] C.-W. Chen, T. Serizawa, M. Akashi, Chem. Mater. 11 (1999) 1381.
[27] S.D. Jackson, G.D. McLellan, G. Webb, L. Conyers, M.B.T. Keegan, S. Mather, S. Simpson, P.B. Wells, D.A. Whan, R. Whyman, J. Catal. 162 (1996) 10.
[28] G. Jacobs, F. Ghadiali, A. Pisanu, A. Borgna, W.E. Alvarez, D.E. Resasco, Appl. Catal. A 188 (1999) 79.
[29] M. Englisch, A. Jentys, J.A. Lercher, J. Catal. 166 (1997) 25.
[30] G. Cocco, R. Campostrini, M.A. Cabras, G. Carturan, J. Mol. Catal. 94 (1994) 299.
[31] H. Hirai, H. Wakabayashi, M. Komiyama, Bull. Chem. Soc. Jpn. 59 (1986) 545.
[32] P. Glaus, H. Hofmeister, J. Phys. Chem. B 103 (1999) 2766.
[33] R. van Hardeveld, F. Hartog, Surf. Sci. 15 (1969) 189.
[34] A. Henglein, B.G. Ershov, M. Malow, J. Phys. Chem. 99 (1995) 14129.
[35] P.L. Gai, M.J. Goringe, J.C. Barry, J. Microscopy 142 (1986) 9.
[36] Y. Li, J. Petroski, M.A. El-Sayed, J. Phys. Chem. 104 (2000) 10956.
[37] Z.L. Wang, J.M. Petroski, T.C. Green, M.A. El-Sayed, J. Phys. Chem. B 102 (1998) 6145.
[38] E. Segal, R.J. Madon, M. Boudard, J. Catal. 52 (1978) 45.
[39] F. Zaera, G.A. Somorjai, J. Am. Chem. Soc. 106 (1984) 228.
[40] G.C. Bond, Catalysis by Metals, Academic Press, New York, 1962, pp. 183–214.
[41] G.A. Somorjai, R. Zaera, J. Phys. Chem. 86 (1982) 3070.
[42] M. Salermon, G.A. Somorjai, J. Phys. Chem. 86 (1982) 341.
[43] G. Cocco, R. Campostrini, M.A. Cabras, G. Carturan, J. Mol. Catal. 94 (1994) 299.
[44] P.H. Otero-Schipper, W.A. Wachter, J.B. Butt, R.L. Burwell, J.B. Cohen, J. Catal. 50 (1977) 494.
[45] Z.L. Wang, T.S. Ahmad, M.A. El-Sayed, Surf. Sci. 380 (1997) 302.
[46] R.E. Benfield, J. Chem. Soc., Faraday Trans. 88 (1992) 1107.
[47] S. Mukerjee, I. McBreen, J. Electroanal. Chem. 448 (1998) 163.
[48] J. Le Bars, U. Specht, J.S. Bradley, D.G. Blackmond, Langmuir 15 (1999) 7621.
[49] J.F. Ciebien, R.E. Cohen, A. Duran, Supramolecular Sci. 5 (1998) 31.
[50] T.S. Ahmadi, Z.L. Wang, T.C. Green, A. Henglein, M.A. El-Sayed, Science 272 (1996) 1924.
[51] M. Liu, W. Yu, H. Liu, J. Zheng, J. Colloid Interface Sci. 214 (1999) 231.
[52] Y. Shiraishi, M. Nakayama, E. Takagi, T. Tominaga, N. Toshima, Inorg. Chim. Acta 300 (2000) 964.
[53] P. Lu, N. Toshima, Bull. Chem. Soc. Jpn. 73 (2000) 751.
[54] C.E. Zinola, C. Gomis-Bas, G.L. Estiu, E.A. Castro, A.J. Arvia, Langmuir 14 (1998) 3091.